UNCLASSIFIED

UNCLASSIFIED
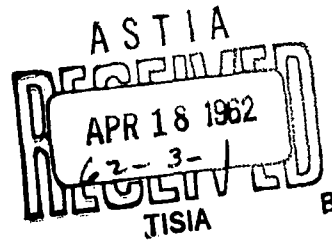
X-RAY INVESTIGATIONS OF Mn_3P, Mn_2P and Ni_2P

Stig Rundqvist

Institute of Chemistry, University of Uppsala Uppsala, Sweden.

Technical Note No. 30
Contract No. AF 61(052)-40
December 27, 1961

X - ray investigations of Mn_3P, Mn_2P, and Ni_2P.

Stig Rundqvist

Institute of Chemistry, University of Uppsala, Uppsala, Sweden.

The crystal structures of Mn_3P (Fe_3P type), Mn_2P and Ni_2P (revised $\underline{C}$ 22 type) have been refined by single-crystal methods. Both Mn_2P and Ni_2P have appreciable homogeneity ranges. X-ray powder investigations in the Mn-P system indicate that the existence of the phase described as Mn_3P_2 is doubtful.

The crystal structures of transition metal phosphides with the compositions Me_3P and Me_2P have been the subject of earlier investigations by the author [1,2,3,4,5] in order to provide material for detailed crystal-chemical comparisons within this group of compounds. In the present paper, accurate structure determinations of Mn_3P, Mn_2P, and Ni_2P are reported. In addition, some phase-analytical data for the Mn-P system are presented and discussed.

Experimental

Preparation. The starting materials for the preparations were electrolytic manganese (AB Ferrolegeringar, Stockholm, claimed purity higher than 99.9%), nickel rods, spectrographically standardized (Johnson, Matthey & Co, Ltd., London), and red phosphorus (purity higher than 99%). Master alloys were prepared by dropping pellets of red phosphorus into molten metal, contained in crucibles of pure alumina (Degussit Al 23 from

Degussa, Frankfurt, Germany). The melting was done by induction heating under a purified argon atmosphere. Alloys of various compositions were made by mixing portions of the crushed master alloys and heating in evacuated and sealed silica tubes. The nickel phosphides did not attack silica appreciably, even after very long heat-treatments. The manganese phosphides, however, attack silica, and the annealing time for manganese phosphides was therefore kept as short as possible.

X-ray work. The phase analyses were performed by X-ray powder methods only. Powder photographs were recorded in Guinier-type focussing cameras with $CrK\alpha_1$ radiation using silicon ($a = 5.4305$ Å) as the internal calibration standard. The accuracy of a single lattice parameter measurement is estimated to be 0.04 %, but lattice parameter differences larger than 0.02 % measured for the same phase in different alloys are probably significant.

Single-crystal fragments with roughly uniform cross-sections not exceeding 0.05 mm were selected from the crushed alloys. Weissenberg photographs were taken using zirconium-filtered MoK radiation. The multiple-film technique, with thin iron foils between successive films, was used. The intensities were estimated visually by comparison with calibrated spots. Corrections for Lorentz and polarisation factors, Fourier series summations, structure factor calculations, and calculations of interatomic distances were made on the electronic digital computer BESK with programmes available at BESK. Atomic scattering factors were taken from tables given for manganese by Watson and Freeman[6], for nickel by Thomas and Umeda [7], and for phosphorus by Tomiie

and Stam [8]. The real part of the dispersion correction for the scattering factors of the atoms as given by Dauben and Templeton [9] was inserted for each of the metal atoms in the structure factor calculations. Standard deviations for the atomic positions were estimated using Cruickshank's [10] equation. (List of observed and calculated structure factors can be obtained from this Institute on request).

The manganese - phosphorus system.

Earlier work on the Mn-P system is summarized by Hansen [11]. X-ray investigations by Årstad and Nowotny [12] showed the existence of Mn_3P, Mn_2P and MnP. Thermal analytical, microscopic, and X-ray investigations by Berak and Heumann [13] confirmed the findings of Årstad and Nowotny, and in addition indicated the existence of Mn_3P_2.

In the present investigation, which is restricted to the range 0-50 atom % phosphorus, the only intermediate phases observed were Mn_3P, Mn_2P and MnP. Within the limits of experimental error, the lattice parameters of Mn_3P and MnP were unchanged in alloys with different compositions and heat-treatments. No appreciable lattice parameter variations for Mn_2P were observed in two-phase Mn_3P + Mn_2P alloys (see Table 1), but variations were observed in alloys containing more than 33 $^1/3$ atom % phosphorus. In order to study this effect more closely, a special investigation of the Mn_2P - MnP part of the system was undertaken. Since the results differ from those obtained by Berak and Heumann, the work will be described in some detail.

A large number of alloys with the composition $Mn_{1.5}P$ were annealed in silica tubes at various temperatures between 800°C

and 1090°C for periods varying from one hour to seven days, and subsequently cooled. The rate of cooling was found to have a marked influence on the final state of the samples, and three different methods of cooling the alloys from the annealing temperature to room temperature were therefore used : 1. cooling in air (room temperature attained in 5-10 minutes), 2. dropping the alloys in water without breaking the silica capsules (room temperature in 10-20 seconds), 3. dropping the alloys in water and breaking the capsules (room temperature in less than 3 seconds). The last method will be referred to as "rapid quenching" in the following text.

The X-ray powder photographs of all these alloys showed that the two phases Mn_2P and MnP alone were present. The MnP diffraction lines were invariably sharp, whereas the Mn_2P lines were more or less diffuse, depending on the cooling rate. The diffraction lines of Mn_2P were quite sharp for rapidly quenched alloys, which had been annealed at temperatures below approximately 1060°C. The unit cell dimensions decreased progressively with increasing annealing temperature (see Table 1). The air-cooled alloys gave rather diffuse Mn_2P lines. The unit cell dimensions were only slightly smaller than those obtained for Mn_2P in two-phase $Mn_3P + Mn_2P$ alloys. The diffraction lines were generally very broad for alloys which had been quenched in water without breaking the silica capsules. In a few cases, two different sets of Mn_2P lines, one sharp and one diffuse, were discernible in the powder photographs of these alloys. For each sharp line, a corresponding diffuse line with a slightly smaller diffraction angle was observed. In some instances, a similar effect was also noticed for rapidly quenched alloys,

which had been annealed at temperatures above $1060^{\circ}C$.

All these observations consistently indicate that Mn_2P has a finite homogenity range, the phosphorus-rich limit of which moves with increasing temperature towards the phosphorus-rich side of the diagram. MnP is precipitated during the cooling of $Mn_{1.5}P$ alloys, while the Mn_2P phase becomes more metal-rich. In rapidly quenched alloys, the secondary precipitation of MnP is negligible. The powder photographs of these alloys exhibit sharp Mn_2P lines. This indicates a well-crystallized condition of the phase, which has the phosphorus-rich limiting composition corresponding to the annealing temperature used. For lower rates of cooling, the secondary precipitation of MnP is appreciable. The broadening of the Mn_2P diffraction lines is attributable to coring effects. In extreme cases, the supercooling may produce the double set of Mn_2P lines referred to above. The set of sharp lines belongs to phosphorus-rich material retained un-decomposed on quenching, while the set of diffuse lines corresponds to more metal-rich Mn_2P which is formed at lower temperatures. The powder photographs exhibit all types of line intermediate between the extremes of very broad lines on the one hand and two separate sets on the other. There is therefore no reason to believe that the double set of lines indicates a two-phase region, in which equilibrium exists between two Mn_2P-type phases of different composition.

As mentioned above, the only phases observed in the range $33\ 1/3$ - 50 atom % P are Mn_2P and MnP. This is in contrast to the report by Berak and Heumann [13] (B & H), who claim the existence of an intermediate phase with the composition Mn_3P_2. This phase is stated to form peritectically at $1090^{\circ}C$ (only $5^{\circ}C$ above

the eutectic temperature) and decompose eutectoidally at 1002°C. The failure to detect any Mn_3P_2 phase in the present investigation may be due to unsuccessful annealing and/or quenching techniques. It is felt, however, that the arguments presented by B & H for the existence of Mn_3P_2 are not convincing. An attempt to reconcile their observations with the present findings can be made as follows.

The thermal arrest at 1002°C observed by B & H (the somewhat scattered experimental points were obtained only on cooling) may be explained by thermal effects, possibly obscured by supercooling, which would accompany the secondary precipitation of MnP from the phosphorus-rich Mn_2P phase. The microscopic examination by B & H of an $Mn_{1.5}P$ alloy, quenched from 1080°C, showed a homogeneous phase together with traces of Mn_2P and MnP. The homogeneous phase, claimed to be the new Mn_3P_2 phase, may in fact have been phosphorus-rich Mn_2P, which had been retained undercomposed on quenching. The powder photograph of a further $Mn_{1.5}P$ alloy, quenched from 1080°C, was stated to contain new lines in addition to the Mn_2P pattern. Since the authors do not claim any high accuracy for their X-ray measurements, and no X-ray data for the new phase were given, it is not unreasonable to believe that their powder photograph contained a double set of Mn_2P lines, possibly in addition to MnP lines. As mentioned before, powder photographs of this type have been obtained by the present author.

The homogeneity range of Ni_2P.

In a previous communication [14] on the nickel-phosphorus system the phase $Ni_{12}P_5$ was described. In the present investigation it was found that there exists a two-phase region $Ni_{12}P_5$ + Ni_2P up to at least $1000^\circ C$. The lattice parameters of Ni_2P were measured in two-phase $Ni_{12}P_5$ + Ni_2P alloys quenched from various temperatures up to $1000^\circ C$. The measured unit cell dimensions dit not show detectable variations and were $\underline{a} = 5.865$ Å, $\underline{c} = 3.387$ Å. These values are significantly larger than those obtained for the single-phase Ni_2P sample used for the single-crystal work (see below). The unit cell dimensions for Ni_2P in the last-mentioned sample were $\underline{a} = 5.859$ Å, $\underline{c} = 3.382$ Å. Ni_2P accordingly exhibits contraction of the unit cell with increasing phosphorus content analoguous to that found for Mn_2P. The equilibria between Ni_2P and more phosphorus-rich intermediate phases are not yet known, and were not studied in the present investigation.

The structure determination of Mn_3P.

According to Årstad and Nowotny [12], Mn_3P is isostructural with Fe_3P. This is confirmed by the present investigation. Weissenberg photographs of Mn_3P were taken with crystals rotated about the $\underline{a}$ and $\underline{c}$ axes. The structure was refined from successive electron density maps and difference maps projected on the $\underline{a}\,\underline{c}$ and $\underline{a}\,\underline{b}$ planes. For the 129 F ($\underline{h}\,\underline{k}\,0$) values observed, the final $\underline{R}$-value of 0.064 was obtained. An overall, isotropic temperature factor with $\underline{B} = 0.44_9$ Å^2 was applied. The corresponding figures for the 92 $\underline{F}$ ($\underline{h}\,0\,\underline{l}$)-values observed were $\underline{R} = 0.048$, $\underline{B} = 0.34_5$ Å^2.

(The very strong (004) reflection was omitted on account of extinction). For each atom, two sets of $\underline{x}$ and $\underline{y}$ parameters were obtained, one from the $\varrho(\underline{x}\ \underline{y})$ and one from the $\varrho(\underline{x}\ \underline{z})$ projection. The final differences between these parameter values did not exceed 0.0005 for any atom. The parameter values quoted below are weighted averages, obtained by giving the values from the centro-symmetric $\underline{x}\ \underline{y}$ projection twice the weight of those from the non-centrosymmetric $\underline{x}\ \underline{z}$ projection.

Final structure data for Mn_3P are as follows:

$$\text{Space group } \underline{I}\ \bar{4} - (\underline{S}\ ^{2}_{4}),\ \underline{Z} = 8$$

$$\underline{a} = 9.181\ \text{Å};\ \underline{c} = 4.568\ \text{Å};\ \underline{U} = 385.0\ \text{Å}.$$

Atoms in 8($\underline{g}$)	$\underline{x}$	$\sigma(\underline{x})$	$\underline{y}$	$\sigma(\underline{y})$	$\underline{z}$	$\sigma(\underline{z})$
Mn_I	0.0807	0.0002	0.1071	0.0002	0.2279	0.0006
Mn_{II}	0.3567	0.0002	0.0319	0.0002	0.9863	0.0006
Mn_{III}	0.1721	0.0002	0.2192	0.0002	0.7531	0.0006
P	0.2935	0.0004	0.0450	0.0004	0.4880	0.0011

Interatomic distances are listed in Table 2.

The structure determinations of Mn_2P and Ni_2P.

Single-crystals of Mn_2P were selected from a two-phase $Mn_3P + Mn_2P$ alloy. Good single-crystals of Ni_2P proved to be more difficult to obtain, since they were found to be very sensitive to mechanical deformation, which resulted in the X-ray patterns

exhibiting elongated and diffuse spots. It was found, however, that crystal fragments picked from crushed alloys gave single-crystals suitable for X-ray work after a 30 minute heat-treatment at $930^{\circ}C$.

The hexagonal Mn_2P and Ni_2P structures both belong to the revised $\underline{C}$ 22 (Fe_2P) structure type [1]. The space group is $\underline{P}\ \bar{6}\ 2\ \underline{m}$ with three metal atoms in 3 ($\underline{f}$), three metal atoms in 3 ($\underline{g}$), two phosphorus atoms in 2 ($\underline{c}$) and one phosphorus atom in 1 ($\underline{b}$). Both structures were refined by successive electron density projections on the basal plane. During the refinements it was found that the temperature factor of the 3 ($\underline{g}$) metal atoms was much higher than that of the 3 ($\underline{f}$) atoms. Individual isotropic temperature factors were therefore introduced, which lowered the $\underline{R}$-value for Mn_2P from 0.058 to 0.045 for the 67 $\underline{F}$ ($\underline{h}\ \underline{k}$ 0)-values observed, and for Ni_2P from 0.075 to 0.063 for the 51 $\underline{F}$ ($\underline{h}\ \underline{k}$ 0)-values observed. Electron counts did not indicate different scattering parameters for the two sets of metal atoms.

Final structure data for Mn_2P are as follows:

Space group $\underline{P}\ \bar{6}\ 2\ \underline{m}$ - ($\underline{D}\ _{3\underline{h}}^{3}$); $\underline{Z}$ = 3

$\underline{a}$ = 6.081 Å; $\underline{c}$ = 3.460 Å; $\underline{U}$ = 110.8 $Å^3$

	$\underline{x}$	$\sigma(\underline{x})$	$\underline{B}$ ($Å^2$)
3 Mn_I in 3 ($\underline{f}$)	0.2546	0.0004	0.23_4
3 Mn_{II} in 3 ($\underline{g}$)	0.5943	0.0004	0.43_0
2 P_I in 2 ($\underline{c}$)			0.40
1 P_{II} in 1 ($\underline{b}$)			0.40

Final data for Ni_2P are as follows:

$\underline{a} = 5.859$ Å; $\underline{c} = 3.382$ Å; $\underline{U} = 100.5$ Å^3

		$\underline{x}$	$\delta(\underline{x})$	$\underline{B}$ (Å^2)
3 Ni_I	in 3 ($\underline{f}$)	0.2575	0.0004	0.32
3 Ni_{II}	in 3 ($\underline{g}$)	0.5957	0.0005	0.69
2 P_I	in 2 ($\underline{c}$)			0.42
1 P_{II}	in 1 ($\underline{b}$)			0.42

The unit cell dimensions for Mn_2P and Ni_2P quoted above were obtained from powder photographs of the alloys from which the single-crystal specimen were selected.

Interatomic distances are given in Table. 3. A description of the $\underline{C}$ 22 structure is given in ref. 1.

Concluding remarks

The substantial homogeneity ranges of Mn_2P and Ni_2P have escaped the notice of previous investigators. In the present author's opinion, the results of Berak and Heumann in the Mn_2P - MnP part of the Mn-P equilibrium diagram may be explained simply by the extended Mn_2P single-phase field without the intro-duction of a new intermediate phase. Clearly, an accurate re-determination of the thermal data for the Mn-P system is desirable.

Extended homogeneity ranges seem to be common in Me_2P-type phosphides. According to Haughton [15], secondary precipitation of

FeP in two-phase Fe_2P + FeP alloys indicates a **wider** homogeneity range for Fe_2P at higher temperatures. The existence of an extended homogeneity range for Co_2P has been demonstrated by Nowotny [16] and by the present author [2], and there are also signs of a similar effect for Ru_2P. Variations of the Fe_2P unit cell dimensions have not been measured, but for Mn_2P, Ni_2P, and Co_2P the unit cell volumes decrease with increasing atomic ratios of phosphorus/ /**metal**. For Co_2P it has been shown [2] that the homogeneity range extends from the stoichiometric composition towards the phosphorus-rich side of the diagram. This is probably due to a varying number of vacancies on one of the crystallographically non-equivalent cobalt atom sites (Co_{II}). The structure of Co_2P is closely related to that of Mn_2P, Fe_2P, and Ni_2P, and the coordination of the Co_{II} atoms is closely similar to that of the Mn_{II}, Fe_{II} and Ni_{II} atoms. (For more detailed descriptions of these structures, see refs. [1, 2]). It is noteworthy that the temperature factors for the Mn_{II} and Ni_{II} atoms are substantially larger than those for Mn_I and Ni_I. The origin of this effect is not easy to explain. However, the effect may indicate that the Mn_{II} and Ni_{II} atomic positions are more likely to be the sites of vacancies or disorder in non-stoichiometric Mn_2P and Ni_2P.

References:

1. Rundqvist, S. and Jellinek, F. Acta Chem. Scand. <u>13</u> (<u>1959</u>) 425.

2. Rundqvist, S.   <u>Ibid.</u>   <u>14</u> (<u>1960</u>)1961.

3. Rundqvist, S.   <u>Ibid.</u>   <u>14</u> (<u>1960</u>)2246.

4. Rundqvist, S.   <u>Ibid.</u>   <u>15</u> (<u>1961</u>) 342.

5. Rundqvist, S.   <u>Ibid.</u>   (in print)

6. Watson, R.E. and Freeman, A.I. <u>Acta Cryst.</u>   <u>14</u> (<u>1961</u>) 27.

7. Thomas, L.H. and Umeda, K.   <u>J.Chem.Phys.</u>   <u>26</u> (<u>1957</u>) 293.

8. Tomiie, Y. and Stam, C.H.   <u>Acta Cryst.</u>   <u>11</u> (<u>1958</u>) 126.

9. Dauben, C.H. and Templeton, D.H.   <u>Ibid.</u>   <u>8</u> (<u>1955</u>) 841.

10. Cruickshank, D.W.J.   <u>Ibid.</u>   <u>2</u> (<u>1949</u>) 65.

11. Hansen, M.   <u>Constitution of Binary Alloys</u>, Mc Graw-Hill,

                   New York-Toronto-London, 1958.

12. Årstad, O. and Nowotny, H. <u>Z.physik.Chem.</u>   <u>B38</u> (<u>1938</u>) 356.

13. Berak, J. and Heumann, Th. <u>Z.Metallkunde</u>   <u>41</u> (<u>1950</u>) 19.

14. Rundqvist, S. and Larsson, E. <u>Acta Chem.Scand.</u>   <u>13</u> (<u>1959</u>) 551.

15. Haughton, J.L.   <u>J. Iron Steel Inst.</u>   <u>115</u> (<u>1927</u>) 417.

16. Nowotny, H.   <u>Z. anorg. Chem.</u>   <u>254</u> (<u>1947</u>) 31.

Table 1. Lattice parameters (in Å) of Mn_2P in two-phase $Mn_3P + Mn_2P$ and $Mn_2P + MnP$ alloys, quenched from various temperatures.

Temp. °C	Two-phase Mn_3P+Mn_2P alloy		Two-phase Mn_2P+MnP alloy	
	a	c	a	c
900	6.081	3.460	6.074	3.451
1000	6.081	3.460	6.068	3.446
1070	6.080	3.458	6.059	3.440

Table. 2. <u>Interatomic distances in Mn_3P (Å)</u>

(Distances shorter than 3.7 Å listed)

	Mn_I	Mn_{II}	Mn_{III}	P
Mn_I	$2.46_2, 2.71_4$ (2), 3.03_5 (2)	$2.69_8, 2.84_9, 3.56_5$	$2.54_3, 2.74_2, 2.77_6, 2.81_9, 2.86_3$	$2.35_7, 2.43_8, 3.56_9$
Mn_{II}	$2.69_8, 2.84_9, 3.56_5$	$2.69_6, 2.88_0(2) 3.07_2(2)$	$2.55_3, 2.60_3, 2.63_9, 3.54_9$	$2.35_2, 2.36_1, 2.36_7, 2.37_0$
Mn_{III}	$2.54_3, 2.74_2, 2.77_6, 2.81_9, 2.86_3$	$2.55_3, 2.60_3, 2.63_9, 3.54_9$	2.75_4 (2)	$2.29_5, 2.37_7, 2.43_7, 3.62_4$
P	$2.35_7, 2.43_8, 3.56_9$	$2.35_2, 2.36_1, 2.36_7, 2.37_0$	$2.29_5, 2.37_7 2.43_7, 3.62_4$	3.50_1 (2) 3.64_1 (2)

Table 3.   Interatomic distances in Mn_2P and Ni_2P (Å)

(Distances shorter than 3.7 Å listed)

Type of distance	Number of equivalent distances	Mn_2P	Ni_2P	Type of distance	Number of equivalent distances	Mn_2P	Ni_2P
Me_I-Me_I	2	2.68_2	2.61_3	P_I-Me_I	3	2.30_4	2.20_9
	2	3.46_0	3.38_2				
Me_I-Me_{II}	2	2.69_4	2.60_5	P_I-Me_{II}	6	2.53_0	2.45_6
	4	2.76_7	2.67_8				
Me_I-P_I	2	2.30_4	2.20_9	P_I-P_I	2	3.46_0	3.38_2
Me_I-P_{II}	2	2.32_2	2.26_6		3	3.51_1	3.38_3
$Me_{II}-Me_{II}$	4	3.19_9	3.08_6	$P_{II}-Me_I$	6	2.32_2	2.26_6
	2	3.46_0	3.38_2				
$Me_{II}-P_I$	4	2.53_0	2.45_6	$P_{II}-Me_{II}$	3	2.46_7	2.36_9
$Me_{II}-P_{II}$	1	2.46_7	2.36_9		3	3.61_4	3.49_0
	1	3.61_4	3.49_0	$P_{II}-P_{II}$	2	3.46_0	3.38_2